

# Structural Rearrangements in Triple-Decker-Like Complexes with Mixed Group 15/16 Ligands: Synthesis and Characterization of the Redox Couple $[\text{Cp}_2^*\text{Fe}_2\text{As}_2\text{Se}_2]/[\text{Cp}_2^*\text{Fe}_2\text{As}_2\text{Se}_2]^+$ ( $\text{Cp}^* = \text{C}_5\text{Me}_5$ )

Olivier Blacque,<sup>[b]</sup> Henri Brunner,<sup>[a]</sup> Marek M. Kubicki,<sup>[b]</sup> Franz Leis,<sup>[a]</sup> Dominique Lucas,<sup>[b]</sup> Yves Mugnier,<sup>[b]</sup> Bernhard Nuber,<sup>[c]</sup> and Joachim Wachter<sup>\*,[a]</sup>

Dedicated to Professor Otto J. Scherer

**Abstract:** The reaction of  $\text{As}_4\text{Se}_4$  with stoichiometric amounts of  $[\text{Cp}_2^*\text{Fe}_2(\text{CO})_4]$  ( $\text{Cp}^* = \text{C}_5\text{Me}_5$ ) in boiling toluene forms  $[\text{Cp}_2^*\text{Fe}_2\text{As}_2\text{Se}_2]$  (**1**) in good yield. X-ray crystallography shows **1** to have a triple-decker structure which comprises a tetraatomic  $\mu, \eta^{4,4}$ - $\text{As}_2\text{Se}_2$  ligand. Density functional theory (DFT) and extended Hückel molecular orbital (EHMO) calculations confirm that the  $\text{As}_2\text{Se}_2$  ligand behaves as a four-electron  $\pi$  donor. Oxidation of **1** with equimolar amounts of  $[(\text{C}_5\text{H}_5)_2\text{Fe}]\text{PF}_6$ ,  $\text{Br}_2$  and  $\text{I}_2$ , respectively, gave compounds **2–4**. According to X-ray crystallographic investigations that were carried out on **2** and

**4**, the oxidation state has a considerable influence on the structure of the  $\text{Fe}_2\text{As}_2\text{Se}_2$  core: significant shortening of the Fe–Fe distance ( $\Delta d(\text{Fe–Fe}) > 0.3 \text{ \AA}$ ) and weakening of the As–As bond length ( $(\Delta d(\text{As–As}) > 0.3 \text{ \AA})$ ) suggests the formal presence of two diatomic AsSe ligands and a Fe–Fe bond. DFT and EHMO calculations confirm that an electron is removed from an occupied Fe–Fe orbital of antibonding character during oxidation. All molec-

ular orbitals lower their energies upon oxidation, but the energy drop is relatively small for those involving the As–As bond. An additional structural feature in **4** consists of an electronic interaction of the iodide with both As atoms which suggests a formally neutral ion pair. Electrochemical studies confirm that the oxidation of **1** is a reversible one-electron process with  $E_{1/2} = +0.07 \text{ V}$  (in THF). These studies also reveal that **4** dissociates in polar solvents, such as THF, into  $[\mathbf{1}]^+$  and  $\text{I}^-$ , which is followed by transformation into **1** and  $\text{I}_3^-$ .

**Keywords:** arsenic • iron • selenium  
• structure elucidation

## Introduction

The chemistry of mixed ligands from Group 15/16 elements represents a rapidly growing field, which ranges from diatomic ligands, which are either unstable in the free state or nonexistent, to polymers in natural and synthetic solids. Anionic and neutral main group clusters lie between these extremes and either serve as ligand precursors or are directly incorporated into metal complexes.<sup>[1, 2]</sup> Suitable substrates for small ligands are organometallic fragments which contain, for example, cyclopentadienyl and/or CO ligands. It is interesting

to compare the structural and electronic properties of the products obtained from complexes derived from pure Group 15 (E)<sup>[3a–d]</sup> or Group 16 (X)<sup>[4a–f]</sup> elements with those obtained from mixed  $\text{E}_m\text{X}_n$  ligands.

The incorporation of diatomic AsS ligands into organometallic complexes has been realized by different methods.<sup>[5a–d]</sup> A related chemistry of AsSe ligands does not yet exist, although selenoarsenates<sup>[6a–c]</sup> and mixed anionic cage molecules<sup>[7a,b]</sup> have been employed for the synthesis of extended structures or molecular “metal main group hybrid clusters”.<sup>[8]</sup> Herein we report the reaction of amorphous  $\text{As}_4\text{Se}_4$  with  $[\text{Cp}_2^*\text{Fe}_2(\text{CO})_4]$  ( $\text{Cp}^* = \text{C}_5\text{Me}_5$ ). Structural and reactivity studies of the resulting products reveal an unprecedented rearrangement within the new  $\text{Fe}_2\text{As}_2\text{Se}_2$  core.

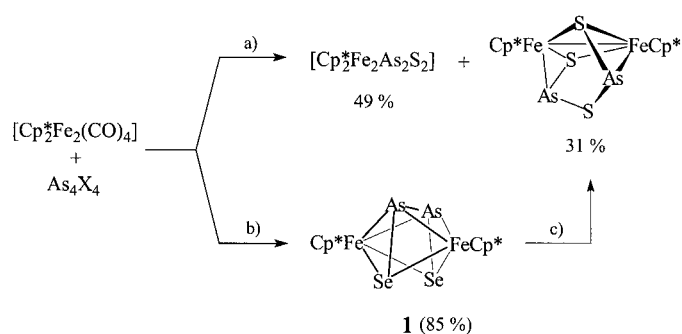
## Results and Discussion

**Synthesis and structure of  $[\text{Cp}_2^*\text{Fe}_2\text{As}_2\text{Se}_2]$  (**1**):** The reaction of  $\text{As}_4\text{Se}_4$  with stoichiometric amounts of  $[\text{Cp}_2^*\text{Fe}_2(\text{CO})_4]$  in boiling toluene gave rise to the green–brown compound  $[\text{Cp}_2^*\text{Fe}_2\text{As}_2\text{Se}_2]$  (**1**) in 85 % yield (Scheme 1 b). The character-

[a] Dr. J. Wachter, Prof. Dr. H. Brunner, Dr. F. Leis  
Institut für Anorganische Chemie der Universität Regensburg  
93040 Regensburg (Germany)  
Fax: (+49)941 9434439  
E-mail: Joachim.Wachter@chemie.uni-regensburg.de

[b] Dr. O. Blacque, Prof. M. M. Kubicki, Dr. D. Lucas, Prof. Y. Mugnier  
Laboratoire de Synthèse et d'Electrosynthèse Organométalliques  
(UMR 5632)  
Université de Bourgogne  
21100 Dijon (France)

[c] Dr. B. Nuber  
Anorganisch-chemisches Institut der Universität Heidelberg  
69120 Heidelberg (Germany)



Scheme 1. a) X = S: toluene, 110 °C; b) X = Se: toluene, 110 °C; c) 1/8 S<sub>8</sub>, CH<sub>2</sub>Cl<sub>2</sub>, 20 °C.

ization of **1** is based on elemental analyses, mass spectrometry and X-ray diffraction studies. The IR spectrum of **1** contains absorption bands typical of the Cp\* ligand. The <sup>1</sup>H NMR spectrum shows a sharp resonance for the methyl groups at  $\delta = 1.45$  and the <sup>77</sup>Se NMR spectrum exhibits a singlet at  $\delta = -388$ .

A slightly different result was obtained some time ago in the analogous reaction of [Cp\*<sub>2</sub>Fe<sub>2</sub>(CO)<sub>4</sub>] with As<sub>4</sub>S<sub>4</sub> in which both [Cp\*<sub>2</sub>Fe<sub>2</sub>As<sub>2</sub>S<sub>2</sub>] and [Cp\*<sub>2</sub>Fe<sub>2</sub>As<sub>2</sub>S<sub>3</sub>] were formed (Scheme 1 a).<sup>[9a,b]</sup> The latter compound was formed in moderate yield in a reaction of **1** with S<sub>8</sub> at room temperature (Scheme 1 c). [Cp\*<sub>2</sub>Fe<sub>2</sub>As<sub>2</sub>S<sub>3</sub>] was identified by its mass spectrum, its typical violet color and its <sup>1</sup>H NMR spectrum. All the data were found to be identical with those of the independently prepared compound.<sup>[9a,b]</sup> The trace product [Cp\*<sub>2</sub>Fe<sub>2</sub>As<sub>2</sub>S<sub>2</sub>Se] was observed which may be derived formally from [Cp\*<sub>2</sub>Fe<sub>2</sub>As<sub>2</sub>S<sub>3</sub>] by substitution of one S by one Se atom.

The reactions presented in Scheme 1 a,b demonstrate a slight but significant difference in the reaction behavior of the As<sub>4</sub>S<sub>4</sub> and As<sub>4</sub>Se<sub>4</sub> starting materials. These differences are more pronounced when the reactions are carried out in toluene at 60 °C. The As<sub>4</sub>Se<sub>4</sub> reaction proceeded more slowly and produced the brown complex [Cp\*<sub>2</sub>Fe<sub>2</sub>(CO)<sub>4</sub>Se<sub>2</sub>]<sup>[10]</sup> as the only product after 14 days, whereas the related As<sub>4</sub>S<sub>4</sub> reaction gave a series of compounds which incorporated As-containing ligands, for example, [Cp\*(CO)<sub>2</sub>FeAs<sub>2</sub>S<sub>2</sub>], which contains the mixed Zintl ion [As<sub>5</sub>S<sub>2</sub>]<sup>-</sup>.<sup>[2, 9a,b, 11]</sup>

A crystal structure determination of **1** shows that its molecular structure (Figure 1) is closely related to that of [(C<sub>5</sub>Me<sub>4</sub>Et)<sub>2</sub>Fe<sub>2</sub>As<sub>2</sub>S<sub>2</sub>].<sup>[9a,b]</sup>

The main group elements form a trapezoid oriented in a parallel manner with respect to the cyclopentadienyl rings of

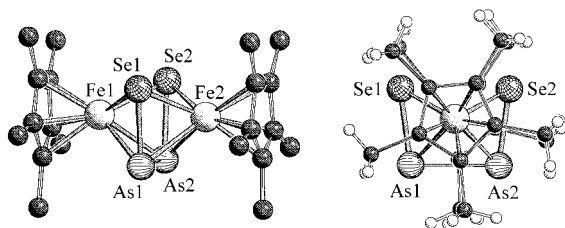


Figure 1. Schakal plots of the molecular structure of **1**.

the organometallic fragments, which bisects the Fe–Fe axis, thus forming a triple-decker-type structure (Figure 1, Table 1).

Table 1. Selected bond lengths [Å] and angles [°] for [Cp\*<sub>2</sub>Fe<sub>2</sub>As<sub>2</sub>Se<sub>2</sub>] (**1**), [Cp\*<sub>2</sub>Fe<sub>2</sub>As<sub>2</sub>Se<sub>2</sub>]PF<sub>6</sub> (**2**) and [Cp\*<sub>2</sub>Fe<sub>2</sub>As<sub>2</sub>Se<sub>2</sub>I] (**4**).

	<b>1</b>	<b>2</b>	<b>4</b>
Fe1...Fe2	3.162(2)	2.821(1)	2.806(2)
Fe1,2–Se1 <sup>[a]</sup>	2.429(4)	2.50(1)	2.410(4)
Fe1,2–Se2 <sup>[a]</sup>	2.413(4)	2.50(1)	2.403(3)
Fe1,2–As1 <sup>[a]</sup>	2.458(4)	2.29(1)	2.383(2)
Fe1,2–As2 <sup>[a]</sup>	2.456(4)	2.28(1)	2.382(6)
As1...As2	2.587(3)	2.89(1)	2.932(3)
Se1–As1	2.279(3)	2.31(1)	2.380(2)
Se2–As2	2.283(3)	2.28(1)	2.364(2)
Se1...Se2	3.198(3)	3.32(1)	3.205(3)
As1...I			3.241(3)
As2...I			3.258(3)
Fe1–Se1,2–Fe2 <sup>[a]</sup>	81.5(1)	76.2(3)	71.3(1)
Fe1–As1,2–Fe2 <sup>[a]</sup>	80.1(1)	68.8(3)	72.2(1)
Se1–As1–As2	98.0(1)	95.0(4)	93.2(1)
Se2–As2–As1	97.3(1)	95.9(4)	93.3(1)
As1–I–As2			53.7(1)

[a] Mean values.

A structural key parameter is the As–As separation which is shorter in **1** (2.587(3) Å) than in [(C<sub>5</sub>Me<sub>4</sub>Et)<sub>2</sub>Fe<sub>2</sub>As<sub>2</sub>S<sub>2</sub>] (2.629(1) Å). A similar trend has been found for the hypothetically naked tetraatomic cisoid planar As<sub>2</sub>X<sub>2</sub> molecules (X = Se: 2.649 Å, X = S: 2.682 Å) by DFT/B3LYP geometry optimizations.<sup>[12]</sup> The observed As–As distances in both iron complexes correspond to values reported for cage molecules like P<sub>2</sub>As<sub>2</sub>S<sub>6</sub> (2.509 Å),<sup>[13]</sup> As<sub>4</sub>Se<sub>4</sub> (2.567(9), 2.57(2) Å),<sup>[14]</sup> β-As<sub>4</sub>S<sub>4</sub> (2.593(6) Å)<sup>[15a-c]</sup> and diarsadisilabicyclo[1.1.0]butane (2.602(3) Å).<sup>[16]</sup> They are, however, longer than those observed or calculated for planar or tetrahedral As<sub>4</sub> units which range from 2.44 to 2.51 Å.<sup>[17]</sup> The As–Se bond lengths in **1** (mean 2.281(3) Å) may have some partial double-bond character like the cyclic anions [As<sub>2</sub>Se<sub>6</sub>]<sup>2-</sup> and [As<sub>3</sub>Se<sub>6</sub>]<sup>3-</sup>, in which exocyclic As–Se bond lengths are between 2.276(2) and 2.296(4) Å as compared to 2.398(3)–2.424(3) Å for endocyclic As–Se.<sup>[18a-d]</sup>

On the basis of these data one may suggest that the Fe<sub>2</sub>As<sub>2</sub>Se<sub>2</sub> core may either contain two coplanar diatomic AsSe bridges (as has been previously assumed for [Cp\*<sub>2</sub>Fe<sub>2</sub>As<sub>2</sub>S<sub>2</sub>]<sup>[2, 9a,b]</sup>) or one μ,η<sup>4-4</sup>-As<sub>2</sub>Se<sub>2</sub> ligand. Free tetraatomic E<sub>2</sub>X<sub>2</sub> molecules are not known with the exception of *cis*-N<sub>2</sub>O<sub>2</sub>,<sup>[19]</sup> but complexes with P<sub>2</sub>X<sub>2</sub> units (X = S,<sup>[20]</sup> Se<sup>[20, 21a,b]</sup>) have been described.

**Electrochemistry and oxidation reactions of [Cp\*<sub>2</sub>Fe<sub>2</sub>As<sub>2</sub>Se<sub>2</sub>] (**1**) and structures of **2** and **4**:** Electrochemical studies show that **1** undergoes two reversible one-electron transfer steps. The cyclic voltammogram of **1** in THF (Figure 2) exhibits two reversible peak systems E<sub>1</sub>/E<sub>1</sub> and E<sub>2</sub>/E<sub>2</sub> between +1 and –1 V. Half-wave potentials (E<sub>1/2</sub> = –0.07 and +0.72 V) were

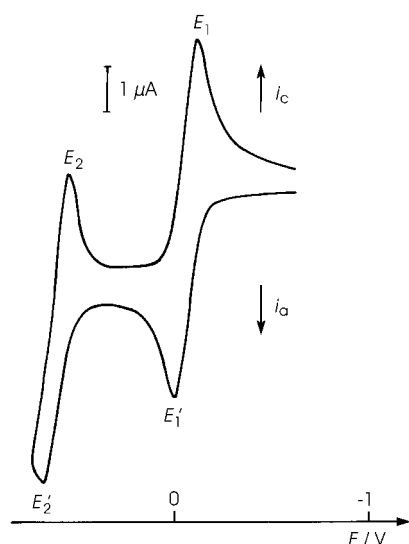


Figure 2. Cyclic voltammogram of **1** ( $c = 1.7 \text{ mmol L}^{-1}$ ) in THF ( $0.2 \text{ mol L}^{-1} \text{ NBu}_4\text{PF}_6$ ) on platinum disk electrode. Sweep rate  $50 \text{ mV s}^{-1}$ , initial potential  $-0.6 \text{ V}$ .

found to increase independently of scan rate and peak currents and linearly with  $v^{1/2}$ . For each oxidation step the potential gap between the anodic and cathodic peaks is close to  $60 \text{ mV}$  (after ohmic drop correction at a scan rate of  $0.05 \text{ V s}^{-1}$ ). This set of data is consistent with two successive one-electron transfer steps.<sup>[22]</sup> The oxidative behavior of **1** has also been studied in  $\text{CH}_2\text{Cl}_2$  on a carbon disk electrode (Figure 3a); similar oxidation features as in THF,  $E_1'$  and  $E_2'$ ,

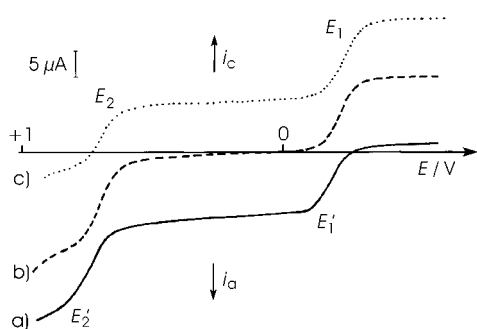
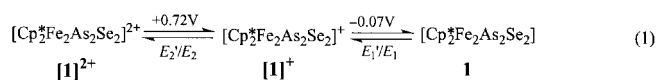


Figure 3. Linear sweep voltammogram of **1** ( $c = 0.8 \text{ mmol L}^{-1}$ ) in  $\text{CH}_2\text{Cl}_2$  ( $0.2 \text{ mol L}^{-1} \text{ NBu}_4\text{PF}_6$ ) on rotating carbon disk electrode. a) At room temperature; b) after oxidation on vitreous carbon gauze at  $0.1 \text{ V}$  ( $Q = 1 \text{ F mol}^{-1}$  of **1**); c) after further oxidation at  $+0.8 \text{ V}$  ( $Q = 1.2 \text{ F mol}^{-1}$  of **1**).

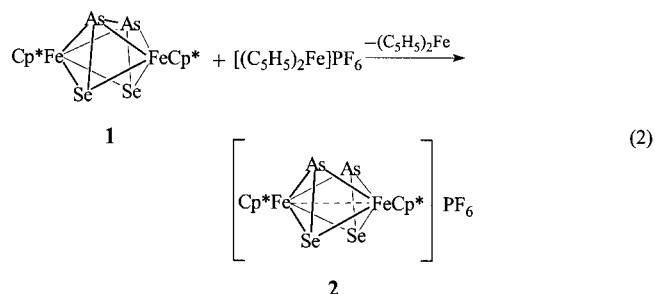
are found, but at slightly more negative potentials ( $E_{1/2} = -0.25$  and  $+0.69 \text{ V}$ ). In addition, we were able to perform electrolyses with the use of carbon as electrode material. Controlled potential electrolysis at  $0.1 \text{ V}$  consumes  $0.95 \text{ F mol}^{-1}$  of **1**. The rotating disk electrode voltammogram of the resulting solution (Figure 3b) shows the oxidation wave  $E_2'$  and reduction wave  $E_1$  according to Equation (1). The



solution of the monocation  $[\mathbf{1}]^+$  exhibits an ESR signal ( $g = 1.9912$ ) with no evidence of coupling with  $^{77}\text{Se}$ . Further

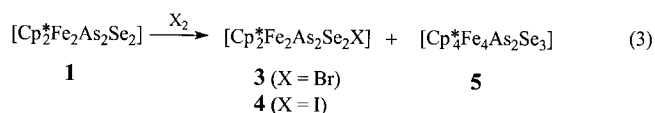
electrolysis at the potential of wave  $E_2'$  (working potential  $+0.8 \text{ V}$ , coulometric consumption of  $1.2 \text{ F mol}^{-1}$  of  $[\mathbf{1}]^+$ ) generates the dication  $[\mathbf{1}]^{2+}$  (Figure 3c) from  $[\mathbf{1}]^+ - e^- \rightarrow [\mathbf{1}]^{2+}$ . However,  $[\mathbf{1}]^{2+}$  is unstable at room temperature and forms  $[\mathbf{1}]^+$  slowly.

Chemical oxidation of **1** with equimolar amounts of  $[(\text{C}_5\text{H}_5)_2\text{Fe}]\text{PF}_6$ ,  $\text{Br}_2$ , and  $\text{I}_2$ , respectively, gave the green–brown compounds **2–4** in good yields [Eqs. (2) and (3)].



Purification of compounds **3** and **4** was achieved by column chromatography on  $\text{SiO}_2$  which suggests that they have some covalent nature. This was confirmed by X-ray crystallographic and electrochemical studies. The composition of compounds **2–4** was confirmed by elemental analyses. The FD mass spectra of **2–4** contain a peak which corresponds to  $[\mathbf{1}]^+$ . The mass spectrum of **4** exhibits an additional peak which may be attributed to the ionized undissociated compound,  $[\text{Cp}_2^*\text{Fe}_2\text{As}_2\text{Se}_2\text{I}]^+$ . This finding is consistent with an iodide ion that is weakly coordinated to the As atoms.

The reaction of **1** with  $\text{I}_2$  also produced trace amounts of brown  $[\text{Cp}_2^*\text{Fe}_4\text{As}_2\text{Se}_3]$  (**5**) [Eq. (3)] which was identified by FD mass spectrometry. One may propose a cubane-like cluster



with a  $\text{Fe}_4(\mu_3\text{-As})_2(\mu_3\text{-Se})_2$  core as a possible structure for **5**, where one As vertex is involved in an *exo* As–Se (third Se atom) double bond.<sup>[20, 23]</sup>

Spectroscopic information on the new compounds **2–4** is relatively poor. Although IR spectra contain  $\nu(\text{C}–\text{H})$  and, in the case of **2**, additional  $\nu(\text{P}–\text{F})$  vibrations, the NMR spectra of the paramagnetic compounds do not show any significant signals. X-ray crystallographic studies have been carried out on single crystals of **2** and **4**.

Complex **2** crystallizes in the centrosymmetric space group  $P\bar{1}$  and contains one discrete organometallic cation  $[\mathbf{1}]^+$  and one  $\text{PF}_6^-$  ion in the unit cell. Thus, the cations occupy a set of special positions around the symmetry centers. This leads to a model with disordered As–Se vectors. Refinement of this model with occupancies of 0.5 for As and Se atoms suggest a trapezoidal geometry of the central tetraatomic unit which is directly derived from that of the parent neutral complex **1** (Figure 4). The As–As bond length in **2** ( $2.89(1) \text{ \AA}$ ) is much longer than in **1** ( $2.587(3) \text{ \AA}$ ) which indicates considerable

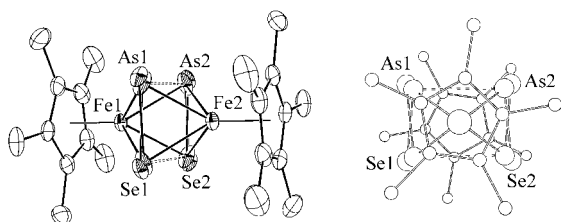


Figure 4. Molecular structure of **2**: Left) ORTEP representation showing the 50% disorder of the main group ligands; right) view along the Fe–Fe vector (Pluto).

weakening or even cleavage of this bond, but it remains shorter than the Se–Se distance (Table 1). The As–Se bond lengths remain essentially unchanged upon oxidation. Another structural feature of interest, which occurs on oxidation of **1** to **2**, is the decrease of the Fe–Fe distance by more than 0.3 Å. This suggests the presence of a metal–metal bond in the cation. The Fe–As bonds in **2** are shorter (mean 2.283 Å) than in **1** (mean 2.457 Å), whereas the Fe–Se bonds are essentially the same (2.438(9) vs. 2.421(3) Å).

The molecular framework of the cation in **4** (Figure 5) resembles roughly those of its precursor **1** and the cation of **2**, although the particular position of the iodide caps almost

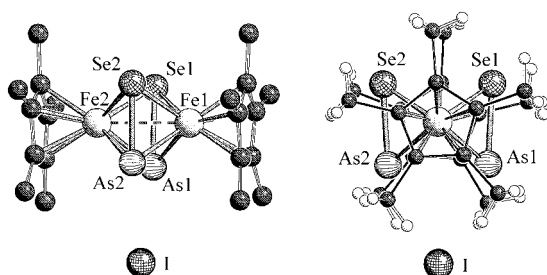


Figure 5. Schakal plots of the molecular structure of **4**.

symmetrically the As–As edge of the (AsSe)<sub>2</sub> middle deck. Nevertheless, significant structural changes and trends within the inorganic cores of **1**, **2** and **4** are observed (Table 1): 1) the Fe–Fe distances decrease in the order **1** > **2** > **4**; 2) the As–As distances increase in the same order; 3) the As–Se bonds in **4** (2.37 Å) are clearly longer than in **1** (2.28 Å) and **2** (2.30 Å); 4) the Se–Se distances vary in the order **1** ≅ **4** < **2**; 5) the Fe–As bond lengths decrease from **1** (2.45 Å) to **4** (2.38 Å) to **2** (2.28 Å) and 6) the Fe–Se bond lengths are longer in **2** (2.50 Å) than in **1** (2.42 Å) and **4** (2.40 Å).

These crystallochemical features argue for a consideration of complex **4** as intermediate between purely ionic and neutral. The iodide anion of compound **4** associates to the molecular frame of the cation [1]<sup>+</sup> which is probably due to its high polarizability. The anion–cation interaction in the resulting neutral adduct is strong enough to allow the purification of **4** (and **3**) by column chromatography. Effectively, the As⋯I contacts (mean distance 3.24 Å) seem to be short enough for significant bonding interactions. For comparison As–I bonds range between 2.51(1) (AsI<sub>3</sub>)<sup>[24]</sup> and 3.051(4) Å (As<sub>6</sub>I<sub>8</sub><sup>2-</sup>).<sup>[25]</sup> An example of van der Waals interactions is found in the AsI<sub>3</sub> lattice, in which the arsenic and iodine layers are separated by about 3.5 Å.<sup>[24]</sup>

The importance of cation–anion interaction to the conformation of the ring methyl groups is evident when viewing the structures of **1**, **2** and **4** along the Fe–Fe vector. The methyl groups in **2** are staggered (Figure 4 right) due to the short Fe–Fe separation, whereas those in **1** (Figure 1 right) and **4** (Figure 5 right) are eclipsed. The eclipsed conformation of Cp\* rings in **4** may be due to the steric effect of iodide interacting with the cation.<sup>[26]</sup>

Electrochemical studies of the halogen-containing compounds **3** and **4** show that they dissociate into discrete ions in CH<sub>2</sub>Cl<sub>2</sub> or THF, which leads to the reduction of [1]<sup>+</sup> by Br<sup>−</sup> or I<sup>−</sup>. Therefore, the resulting solutions contain **1**, [1]<sup>+</sup>, and X<sub>3</sub><sup>−</sup> (X = Br, I). The polarogram of **4** in THF (Figure 6) exhibits

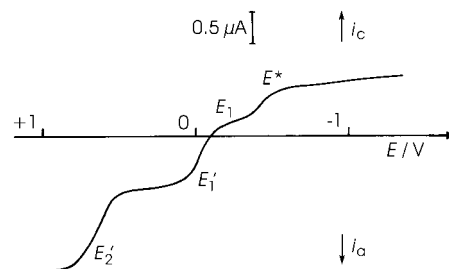
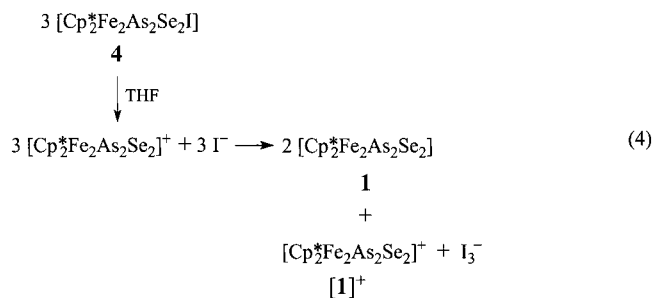


Figure 6. Polarogram (average current) of **4** ( $c = 0.7 \text{ mmol L}^{-1}$ ) in THF ( $0.2 \text{ mol L}^{-1} \text{ NBu}_4\text{PF}_6$ ).

oxidation waves  $E_1'$  and  $E_2'$  and a reduction wave  $E_1$  which demonstrates the presence of both **1** and [1]<sup>+</sup> in solution. An additional reduction wave  $E^*$  is observed at  $-0.44 \text{ V}$  which corresponds to the reduction of I<sub>3</sub><sup>−</sup>.<sup>[27]</sup> The overall process is expressed in Equation (4). The relative heights of waves  $E_1'$  and



$E_1$  (Figure 6) in our experiments show that concentrations of **1** and [1]<sup>+</sup> are effective in a ratio 2:1. This is confirmed by coulometric measurements. Moreover, we have verified that iodide ions act as reducing agents by adding one equivalent of Bu<sub>4</sub>NI to electrogenerated **2**, which incorporates cation [1]<sup>+</sup>, giving rise to the same polarogram as that of Figure 6.

**Theoretical considerations:** Complexes **1–4** may be described as triple-decker-type compounds with mixed ligands from main Groups 15 and 16. A variety of complexes with homoatomic ligands of the type [Cp<sub>2</sub>M<sub>2</sub>E<sub>4</sub>] is known for E = P, As, and S and different metals M. Usually, the main group atoms arrange to form rectangles in which diatomic ligands are separated from each other by distances that are too long for strong bonding interactions. Rectangular core geometries with short and long E–E distances have been realized in [(Cp\*Co)<sub>2</sub>P<sub>4</sub>],<sup>[28]</sup> [(C<sub>5</sub>Me<sub>4</sub>EtRh)<sub>2</sub>P<sub>4</sub>],<sup>[29]</sup> [(C<sub>5</sub>Me<sub>5</sub>–

$(\text{Co})_2\text{As}_4$ ]<sup>[30]</sup> and  $[(\text{Cp}^*\text{Fe})_2\text{S}_4]\text{I}_2$ .<sup>[31a,b]</sup> Exceptions include  $[(\text{C}_5\text{Me}_4t\text{BuCo})_2\text{As}_4]^{2+}$  which has an almost square  $\text{As}_4$  middle deck<sup>[17]</sup> and  $[(1,3-t\text{Bu}_2\text{C}_5\text{H}_3\text{Fe})_2\text{P}_4]$ , in which the P atoms form a trapezoid.<sup>[32a,b]</sup> The latter complex shows a dynamic <sup>31</sup>P NMR spectrum in solution which has been interpreted as a rearrangement into a compound with the elusive  $\text{Fe}_2(\mu, \eta^{2-2}\text{P}_2)_2$  core.<sup>[28]</sup>

The geometrical features of complexes **1**, **2** and **4** indicate a contribution of  $\pi$  molecular orbitals of the As/Se bridging ligands to the bonding in these bimetallic complexes. Thus, the  $\text{As}_2\text{Se}_2$  ligand in **1** would behave as a formal four-electron  $\pi$   $\mu, \eta^{4,4}$ -donor giving rise to 30 valence electrons ( $2 \times 13$  (CpFe) + 4 ( $\pi$ )). According to the Wade–Mingos rules<sup>[33a,b]</sup> there are 16 electrons (8 skeleton electron pairs (SEP)) available for cage bonding. This corresponds to a *nido*-pentagonal bipyramid, in which the vacant site is located in the  $\text{As}_2\text{Se}_2$  plane between the selenium atoms. Fourteen of the total 16 electrons are furnished by the  $\text{As}_2\text{Se}_2$  ligand ( $2 \times 3$  As +  $2 \times 4$  Se) and the remaining two electrons are provided by the two CpFe organometallic fragments.

We have carried out the single-point DFT/B3LYP (3–21G basis) (Gaussian94<sup>[34]</sup>) and EHMO (CACAO<sup>[35a,b]</sup>) calculations on **1** ( $\text{C}_5\text{H}_5$  instead of  $\text{C}_5\text{Me}_5$ ) and on the  $\text{As}_2\text{Se}_2$  and CpFe...FeCp fragments where compound **1** was built with idealized  $C_{2v}$  symmetry (Fe–Fe vector taken as “y” direction) and metric parameters from its X-ray data.

These calculations confirm the contribution of 14 electrons from the  $\text{As}_2\text{Se}_2$  central deck to the bonding in **1** (Figure 7). They populate the  $\sigma$  (10 electrons; As–Se and As–As bonds and Se lone pairs) and  $\pi$  (4 electrons; AsSe) molecular

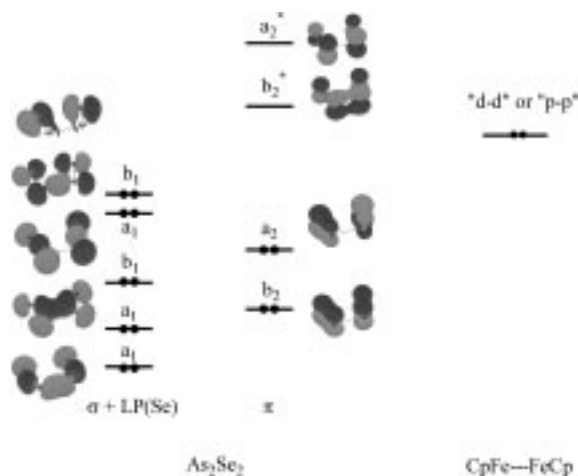


Figure 7. Molecular orbitals relevant for cage bonding in **1**.

orbitals which are built of “p” As and Se atomic orbitals. In agreement with earlier description of the electronic structures of triple deckers<sup>[17,36]</sup>, the two electrons from the naked bimetallic CpFe...FeCp fragment ( $\text{Fe}^1$ ,  $d^7$ ) have “ $d_{xy} - d_{yz}$ ” nature in EHMO calculations. B3LYP/3-21G calculations give the highest occupied molecular orbital (HOMO) of this fragment which is built of a favorable overlap between the “ $sp_y$ ” hybrids from each iron center. Since there is a rather long Fe–Fe separation (3.16 Å), a population of “p” metallic orbitals is plausible for the naked bimetallic CpFe...FeCp

fragment. A further “p–d” rehybridization in this fragment should occur upon complex formation with the tetraatomic  $\text{As}_2\text{Se}_2$  central fragment.

The stability of **1** is not only due to the  $\mu, \eta^{4,4}$  donor nature of the central ligand. There are also strong  $\pi$  back interactions between the  $a_2$ - and  $b_2$ -filled bimetallic orbitals and the empty  $\pi^*$  orbitals of  $\text{As}_2\text{Se}_2$ . Moreover, this stability is enhanced by participation of the in-plane  $\sigma$   $\text{As}_2\text{Se}_2$  orbitals to the overall bonding, which has been discussed by Mealli et al. for complexes with a *cyclo*- $\text{P}_3$  central deck.<sup>[37]</sup>

It has been already stated that the oxidation of **1** leads to a drastic shortening of Fe–Fe distance and a lengthening of As–As bond (Table 1) while retaining the  $\text{Fe}_2\text{As}_2\text{Se}_2$  cage geometry. To improve our understanding of these observations, we have carried out single-point calculations on the cation of **1** with metric parameters from X-ray data found for compound **2** which have been averaged to  $C_{2v}$  symmetry. A comparison of the results obtained for **1** and for the cation of **2** shows that the oxidation occurs mainly at the metal–metal antibonding orbital of  $b_2$  symmetry, which is (for **1**) the HOMO in EHMO calculations and the HOMO-5 in the DFT/B3LYP model. The other higher energy filled orbitals (HOMO to HOMO-4) in the DFT model are nonbonding bimetallic combinations. The  $b_2$  orbital is a current  $\sigma$  metal–metal antibonding  $y^2 - y^2$  function where the “y” direction is taken as that of the Fe–Fe vector. It seems to play a major role in determination of direct metal–metal interactions (and distances) in CpM triple deckers despite other lower energy M–ligand–M bonding interactions. The population of this  $b_2$  orbital by two electrons as in compound **1** (Fe–Fe = 3.16 Å) or in isoelectronic complexes  $[(\text{Cp}^*\text{Co})_2\text{E}_4]$  (Co–Co when E = P: 3.10 Å;<sup>[28]</sup> E = As: 3.19 Å<sup>[30]</sup>) results in M–M distances of nonbonding character. One-electron oxidation reduces this distance to 2.81–2.82 Å as observed in complexes **2** and **4** where the  $b_2$  molecular orbital becomes the HOMO and is occupied by one electron in both EHMO and DFT methods. Non-occupation of this orbital (which becomes the LUMO) leads to the formation of a strong metal–metal bond as observed in  $[(\text{Cp}'\text{Fe})_2\text{P}_4]$  complexes (2.58–2.64 Å).<sup>[28, 32a,b]</sup>

The oxidation of **1** leads to the predicted lowering of the energies of all filled molecular orbitals calculated for the cation of **2**. However, the magnitude of the energy drop for orbitals with As–As bonding nature is smaller than for the other orbitals (with the exception of the  $b_2$  Fe–Fe orbital which was discussed above) and may argue for the observed weakening of the As–As bond in **2**.

The iodide ion in the structure of **4** caps the As–As edge of the  $\text{As}_2\text{Se}_2$  ligand at van der Waals contacts with the As atoms. To recognize whether such a position is a consequence of crystal packing or of an electronic interaction of  $\text{I}^-$  with the cation  $[\mathbf{1}]^+$ , we have carried out single-point calculations on **1**,  $[\mathbf{1}]^+\text{I}^-$  (complex **4**) and  $[\mathbf{1}]^+$  (B3LYP/3–21G, metric parameters from X-ray data) with natural bond orbital (NBO) analyses.<sup>[34]</sup> The trends of charge evolution on different fragments ((CpFe)<sub>2</sub>,  $\text{As}_2\text{Se}_2$ , As, Se) on going from **1** to  $[\mathbf{1}]^+\text{I}^-$  and to  $[\mathbf{1}]^+$  have been evaluated. They gave the following results which are listed in the order **1**,  $[\mathbf{1}]^+\text{I}^-$  and  $[\mathbf{1}]^+$ : +3.26, +2.00, +3.94 for (CpFe)<sub>2</sub>; –3.25, –1.53, –2.94 for  $\text{As}_2\text{Se}_2$ ; –0.58, 0.00, –0.40 for As; –1.04, –0.75, –1.06

for Se. The charge calculated for the iodide in  $[\mathbf{1}]^+ \text{I}^-$  is equal to  $-0.49 e$ . These results show that there is an efficient transfer of electron density from the iodide to the cation  $[\mathbf{1}]^+$  which leads to a true ion pair  $[\mathbf{1}]^+ - \text{I}^-$ . Moreover, the crystals of  $\mathbf{3}$  ( $[\mathbf{1}]^+, \text{Br}^-$ ) are isostructural with  $\mathbf{4}$ .<sup>[26]</sup> A similar cation–anion interaction may take place in the less polarizable bromide.

## Conclusion

The reaction of  $[\text{Cp}_2^*\text{Fe}_2(\text{CO})_4]$  with  $\text{As}_4\text{Se}_4$  gives  $[\text{Cp}_2^*\text{Fe}_2\text{As}_2\text{Se}_2]$  ( $\mathbf{1}$ ) which comprises the novel  $\text{Se}=\text{As}-\text{As}=\text{Se}$  ligand. The result confirms that amorphous  $\text{As}_4\text{Se}_4$  is a convenient source of mixed Group 15/16 ligands.<sup>[38]</sup> Better selectivity of the reaction and pronounced stability of the product as compared to the related  $\text{As}_4\text{S}_4$  reaction allows a detailed investigation of the chemical behavior of  $\mathbf{1}$ , and provides new insights into the structure and bonding of this type of compound. The structural description of  $\mathbf{1}$  on the basis of crystallographic and theoretical investigations is best rationalized as a triple-decker-type complex containing a  $\mu, \eta^{4,4}$ - $\text{As}_2\text{Se}_2$  ligand acting as a four-electron  $\pi$  donor with  $\pi$  back interactions and with contribution of the in-plane  $\sigma$  orbitals of the central deck in the metal–ligand bonding. A previous structural proposal which considered the analogous  $[\text{Cp}_2^*\text{Fe}_2\text{As}_2\text{S}_2]$  to contain two diatomic AsS ligands<sup>[9a,b]</sup> needs therefore to be reconsidered.

Two diatomic AsSe ligands seem to be present in the oxidation products  $\mathbf{2}$ – $\mathbf{4}$  of  $\mathbf{1}$ . Analyses of the electronic situation of  $\mathbf{2}$  show that the As–As interaction persists, though much weaker than in  $\mathbf{1}$ . The case is still more complicated when using  $\text{I}_2$  (or  $\text{Br}_2$ )<sup>[26]</sup> as an oxidant. Structural, electrochemical, and theoretical analyses of  $\mathbf{4}$  evoke similar structural effects as in  $\mathbf{2}$ . However, in the case of  $\mathbf{4}$ , the considerable bonding interactions of the anion with both As atoms of the cation significantly modify the distribution of electron density over the whole molecule.

From a formal point of view the redox couple  $[\text{Cp}_2^*\text{Fe}_2\text{As}_2\text{Se}_2]/[\text{Cp}_2^*\text{Fe}_2\text{As}_2\text{Se}_2]^+$  may be regarded as first example for a reversible dimerization of diatomic EX ligands. In the case of  $\text{E}_4\text{X}_4$  cage fragmentation, however, one has to consider the extrusion of tetraatomic  $\text{E}_2\text{X}_2$  fragments from the cages as new building blocks.<sup>[2]</sup>

## Experimental Section

General methods and instruments that were used have been described in ref. [9]. The ESR spectrum was taken at room temperature on a Bruker ESP300 spectrometer (field calibration with DPPH ( $g = 2.0034$ )). Cyclic voltammetry was carried out in a standard three-electrode Tacussel UAP4 unit cell. The reference electrode was saturated calomel (SCE) separated from the solution by a sintered glass disk. The auxiliary electrode was a Pt wire. For all voltammetric measurements the working electrode was a carbon or Pt disk electrode initially polished with alumina. For the polarograms a three-electrode Tipol polarograph was used. The dropping Hg electrode (DMF) characteristics were  $m = 3 \text{ mg s}^{-1}$  and  $\tau = 0.5 \text{ s}$ . In all cases the electrolyte was a 0.2 M solution of  $n\text{Bu}_4\text{NPF}_6$  in THF or  $\text{CH}_2\text{Cl}_2$ . The electrolyses were performed with an Amel 552 potentiostat coupled to an Amel 721 electronic integrator.

$\text{As}_4\text{Se}_4$  was employed as amorphous powder which was obtained by fusing together equimolar amounts of As and Se at  $500^\circ\text{C}$ .<sup>[14, 39]</sup>

**Synthesis of  $[\text{Cp}_2^*\text{Fe}_2\text{As}_2\text{Se}_2]$  ( $\mathbf{1}$ ):** A grey to violet mixture of  $[\text{Cp}_2^*\text{Fe}_2(\text{CO})_4]$  (494 mg, 1.0 mmol) and  $\text{As}_4\text{Se}_4$  (616 mg, 1.0 mmol) in toluene (50 mL) was refluxed for 15 h. After cooling and filtration the solvent was removed under vacuum. The brown oily residue was dissolved in toluene/pentane (2:1) and chromatographed on silica gel (column  $23 \times 3 \text{ cm}$ ). A green-brown band was eluted in toluene/pentane (2:1) which contained  $\mathbf{1}$  in 85% yield. Recrystallization of  $\mathbf{1}$  from toluene gave dark brown prisms. Elemental analysis calcd (%) for  $\text{C}_{20}\text{H}_{30}\text{As}_2\text{Fe}_2\text{Se}_2$  ( $\mathbf{1}$ ; 689.9): C 34.81, H 4.38; found C 34.58, H 4.50; FD MS (from toluene):  $m/z$  692.1 ( $^{80}\text{Se}$ );  $^1\text{H}$  NMR (250 MHz,  $\text{CDCl}_3$ ,  $25^\circ\text{C}$ , TMS):  $\delta = 1.45$  (s, 30H);  $^{77}\text{Se}$  NMR (76 MHz,  $\text{CDCl}_3$ ,  $\text{Se}(\text{CH}_3)_2$ ):  $\delta = -388$ .

**Synthesis of  $[\text{Cp}_2^*\text{Fe}_2\text{As}_2\text{Se}_2]\text{PF}_6$  ( $\mathbf{2}$ ):** A mixture of  $\mathbf{1}$  (340 mg, 0.49 mmol) and  $[(\text{C}_5\text{H}_5)_2\text{Fe}]\text{PF}_6$  (162 mg, 0.49 mmol) in  $\text{CH}_2\text{Cl}_2$  (80 mL) was stirred for 16 h at  $20^\circ\text{C}$ . After evaporation of the solvent the green-brown residue was suspended in toluene, transferred onto a frit and washed with toluene ( $5 \times 10 \text{ mL}$ ) to remove the yellow ferrocene. The residue was dissolved in  $\text{CH}_2\text{Cl}_2$  (20 mL) and after evaporation of the solvent, crude  $\mathbf{2}$  was obtained in 94% yield. The compound was recrystallized from acetone. Elemental analysis calcd (%) for  $\text{C}_{20}\text{H}_{30}\text{As}_2\text{F}_6\text{Fe}_2\text{PSe}_2$  ( $\mathbf{2}$ ; 834.9): C 28.70, H 3.61; found C 28.38, H 3.69; FD MS (from acetone):  $m/z$  691.7 ( $[\mathbf{1}]^+$ ).

**Synthesis of  $[\text{Cp}_2^*\text{Fe}_2\text{As}_2\text{Se}_2\text{Br}]$  ( $\mathbf{3}$ ):** A solution of  $\text{Br}_2$  (46.3 mg, 0.29 mmol) in  $\text{CHCl}_3$  (0.75 mL) was dropped into the solution of  $\mathbf{1}$  (200 mg, 0.29 mmol) in  $\text{CHCl}_3$  (50 mL). The mixture was stirred for 16 h at  $20^\circ\text{C}$ . After evaporation of the solvent the residue was suspended in toluene (20 mL), filtered over a frit and washed with toluene. The residue was dissolved in acetone and then the solvent was evaporated in vacuo. Chromatography of the residue on silica gel (column  $15 \times 3 \text{ cm}$ ) produced a bright green band, which contained very small quantities of a still unknown product, and a green-brown band, which contained  $\mathbf{3}$  in 78% yield, after elution with toluene/acetone (1:1). Crystals of  $\mathbf{3}$  were obtained from methanol at  $-25^\circ\text{C}$ . Elemental analysis calcd (%) for  $\text{C}_{20}\text{H}_{30}\text{As}_2\text{BrFe}_2\text{Se}_2$  ( $\mathbf{3}$ ; 769.8): C 31.20, H 3.93; found C 31.08, H 4.02; FD MS (from methanol):  $m/z$ : 691.7 ( $[\mathbf{1}]^+$ ).

**Reaction of  $[\text{Cp}_2^*\text{Fe}_2\text{As}_2\text{Se}_2]$  ( $\mathbf{1}$ ) with iodine:** A solution of  $\text{I}_2$  (74 mg, 0.29 mmol) in toluene (10 mL) was slowly added dropwise to the solution of  $\mathbf{1}$  (200 mg, 0.29 mmol) in toluene (40 mL). The mixture was stirred for 16 h at  $20^\circ\text{C}$  and the solvent was then evaporated. The residue underwent chromatography on a silica gel column ( $15 \times 3 \text{ cm}$ ) from which a green band which contained  $[\text{Cp}_2^*\text{Fe}_2(\text{AsSe})_2\text{I}]$  ( $\mathbf{4}$ ) in 84% yield was eluted in toluene/acetone (1:1). A brown band containing  $[\text{Cp}_4^*\text{Fe}_4\text{As}_2\text{Se}_2]$  ( $\mathbf{5}$ ) in 2% yield was eluted with acetone. Crystals of  $\mathbf{4}$  and  $\mathbf{5}$  were obtained by recrystallization from acetone. Elemental analysis calcd (%) for  $\text{C}_{20}\text{H}_{30}\text{As}_2\text{Fe}_2\text{ISe}_2$  ( $\mathbf{4}$ ; 816.8): C 29.34, H 3.69; found C 29.13, H 3.84; FD MS (from acetone):  $m/z$ : 691.9 ( $[\mathbf{1}]^+$ ) and 818.6 ( $[\mathbf{4}]^+$ ). Molecular weight calcd for  $\text{C}_{40}\text{H}_{60}\text{As}_2\text{Fe}_4\text{Se}_3$  ( $\mathbf{5}$ ); 1153.8; FD MS (from acetone):  $m/z$ : 1151.7 (centre, simulated,  $[\mathbf{M}]^+$ ).

**Reaction of  $[\text{Cp}_2^*\text{Fe}_2\text{As}_2\text{Se}_2]$  ( $\mathbf{1}$ ) with  $\text{S}_8$ :** A mixture of  $\mathbf{1}$  (295 mg, 0.43 mmol) and  $\text{S}_8$  (13 mg, 0.43 mmol) in  $\text{CH}_2\text{Cl}_2$  (50 mL) was stirred for 40 h at  $20^\circ\text{C}$ . After evaporation of solvent, the brown residue was applied to a silica gel column ( $15 \times 3 \text{ cm}$ ). The green-brown  $\mathbf{1}$  was recovered in toluene before a red-violet band which contained  $[\text{Cp}_2^*\text{Fe}_2\text{As}_2\text{S}_3]$ <sup>[9]</sup> in 8% yield. Molecular weight calcd for  $\text{C}_{20}\text{H}_{30}\text{As}_2\text{Fe}_2\text{S}_3$ : 628.2; FD MS (from toluene):  $m/z$  627.9 and 675.9 (fitting for  $\text{C}_{20}\text{H}_{30}\text{As}_2\text{Fe}_2\text{S}_2\text{Se}$ )  $[\mathbf{M}]^+$ .

**X-ray structure determination of complexes  $\mathbf{1}$ ,  $\mathbf{2}$  and  $\mathbf{4}$ :**<sup>[40]</sup> Crystal data were collected on a SyntexR3 ( $\mathbf{1}$ ,  $\mathbf{4}$ ) and on an Enraf-Nonius-CAD4 ( $\mathbf{2}$ ) diffractometer at room temperature. Relevant crystal and data collection parameters are summarized in Table 2. The structures were solved by using standard Patterson methods, least-squares refinement, and Fourier techniques. The calculations were performed with the SHELXTL Plus for  $\mathbf{1}$  and  $\mathbf{4}$  (refinement on  $F$ ) and with SHELXL97 for  $\mathbf{2}$  (refinement on  $F^2$ ) program packages.

## Acknowledgement

We are grateful to the Deutsche Forschungsgemeinschaft for financial support of this work and to Prof. Dr. G. Huttner for support of X-ray crystallographic work (structure solution of  $\mathbf{1}$  and  $\mathbf{4}$ ). Parts of this work have also been supported by the Deutscher Akademischer Auslandsdienst (DAAD) and EGIDE of the French government (Procope Program).

Table 2. Crystal structure data of complexes **1**, **2**, and **4**.

	<b>1</b>	<b>2</b>	<b>4</b>
formula	C <sub>20</sub> H <sub>30</sub> As <sub>2</sub> Fe <sub>2</sub> Se <sub>2</sub>	C <sub>20</sub> H <sub>30</sub> As <sub>2</sub> F <sub>6</sub> Fe <sub>2</sub> PSe <sub>2</sub>	C <sub>20</sub> H <sub>30</sub> As <sub>2</sub> Fe <sub>2</sub> ISe <sub>2</sub>
molecular mass	691.8	834.87	818.72
crystal size [mm]	0.40 × 0.55 × 0.70	0.25 × 0.25 × 0.15	0.40 × 0.60 × 0.75
crystal system	monoclinic	triclinic	monoclinic
space group (no.)	<i>P</i> 2 <sub>1</sub> / <i>c</i> (14)	<i>P</i> $\bar{1}$ (2)	<i>P</i> 2 <sub>1</sub> / <i>c</i> (14)
<i>a</i> [Å]	10.541(3)	7.988(1)	14.150(3)
<i>b</i> [Å]	13.736(4)	8.350(1)	10.333(2)
<i>c</i> [Å]	16.655(4)	10.483(1)	16.991(5)
$\alpha$ [°]		98.74(1)	
$\beta$ [°]	103.92(2)	101.40(1)	91.39(2)
$\gamma$ [°]		93.43(1)	
<i>V</i> [Å <sup>3</sup> ]	2341	674.6(1)	2484(1)
<i>Z</i>	4	1	4
$\rho_{\text{calcd}}$ [g cm <sup>-3</sup> ]	1.96	2.06	2.18
<i>F</i> (000)	1344	405	1556
radiation	MoK $\alpha$	MoK $\alpha$	MoK $\alpha$
$\mu$ [mm <sup>-1</sup> ]	7.16	6.32	7.99
scan mode	$\omega$	$\omega$	$\omega$
2 $\theta_{\text{max}}$ [°]	58.0	52.6	50.0
absorption correction ( $\Psi$ scans)	7.0 < 2 $\theta$ < 37.0 (6 reflections)	7.0 < 2 $\theta$ < 39.2 (7 reflections)	7.4 < 2 $\theta$ < 42.6 (8 reflections)
transmission (min/max)	0.52/1.00	0.62/1.00	0.56/1.00
total reflections	6523	2729	4822
observed reflections	2327	1989	2970
	<i>I</i> > 2.5 $\sigma$ ( <i>I</i> )	<i>I</i> > 2.0 $\sigma$ ( <i>I</i> )	<i>I</i> > 2.5 $\sigma$ ( <i>I</i> )
parameters refined	236	166	245
<i>R</i> ( <i>F</i> )	0.085	0.040	0.051
<i>R</i> <sub>w</sub>	0.069	0.103 ( <i>wR</i> ( <i>F</i> <sup>2</sup> ))	0.046
residual electron density [eÅ <sup>-3</sup> ]	+1.17/−1.07	+0.58/−0.75	+1.13/−1.03

- [1] G. W. Drake, J. W. Kolis, *Coord. Chem. Rev.* **1994**, *137*, 131.
- [2] J. Wachter, *Angew. Chem.* **1998**, *110*, 783; *Angew. Chem. Int. Ed.* **1998**, *37*, 750.
- [3] a) K. H. Whitmire, *J. Coord. Chem.* **1988**, *17*, 95; b) D. Fenske, J. Ohmer, J. Hachgenei, K. Merzweiler, *Angew. Chem.* **1988**, *100*, 1300; *Angew. Chem. Int. Ed.* **1988**, *27*, 1277; c) O. J. Scherer, *Angew. Chem.* **1990**, *102*, 1137; *Angew. Chem. Int. Ed. Engl.* **1990**, *29*, 1104; d) A.-J. DiMaio, A. L. Rheingold, *Chem. Rev.* **1990**, *90*, 169.
- [4] a) H. Vahrenkamp, *Angew. Chem.* **1975**, *87*, 363; *Angew. Chem. Int. Ed. Engl.* **1975**, *14*, 322; b) A. Müller, W. Jaegermann, J. H. Enemark, *Coord. Chem. Rev.* **1982**, *46*, 245; c) M. Draganjac, T. B. Rauchfuss, *Angew. Chem.* **1985**, *97*, 745; *Angew. Chem. Int. Ed. Engl.* **1985**, *24*, 742; d) A. Müller, E. Diemann, *Adv. Inorg. Chem.* **1987**, *31*, 89; e) J. Wachter, *Angew. Chem.* **1989**, *101*, 1645; *Angew. Chem. Int. Ed. Engl.* **1989**, *28*, 1613; f) L. C. Roof, J. W. Kolis, *Chem. Rev.* **1993**, *93*, 1037.
- [5] a) H. Brunner, H. Kauermann, U. Klement, J. Wachter, T. Zahn, M. L. Ziegler, *Angew. Chem.* **1985**, *97*, 122; *Angew. Chem. Int. Ed. Engl.* **1985**, *24*, 132; b) A.-J. DiMaio, A. L. Rheingold, *Inorg. Chem.* **1990**, *29*, 798; c) B. K. Das, M. G. Kanatzidis, *Inorg. Chem.* **1995**, *34*, 6505; d) H. Brunner, H. Kauermann, L. Poll, B. Nuber, J. Wachter, *Chem. Ber.* **1996**, *129*, 657.
- [6] a) J.-H. Chou, M. G. Kanatzidis, *J. Solid State Chem.* **1996**, *123*, 115; b) M. G. Kanatzidis, J.-H. Chou, *J. Solid State Chem.* **1996**, *127*, 186; c) J.-H. Chou, J. A. Hanko, M. G. Kanatzidis, *Inorg. Chem.* **1997**, *36*, 4.
- [7] a) T. M. Martin, P. T. Wood, G. L. Schimek, W. T. Pennington, J. W. Kolis, *Inorg. Chem.* **1995**, *34*, 4385; b) S. C. O'Neal, W. T. Pennington, J. W. Kolis, *Inorg. Chem.* **1992**, *31*, 888.
- [8] J. W. Kolis, P. M. Young, *Chemistry, Structure, and Bonding of Zintl Phases and Ions* (Ed.: S. M. Kauzlarich), VCH, **1996**, 225.
- [9] a) H. Brunner, H. Kauermann, B. Nuber, J. Wachter, M. L. Ziegler, *Angew. Chem.* **1986**, *98*, 551; *Angew. Chem. Int. Ed. Engl.* **1986**, *25*, 557; b) H. Brunner, L. Poll, J. Wachter, B. Nuber, *J. Organomet. Chem.* **1994**, *471*, 117.
- [10] W. A. Herrmann, J. Rohrmann, E. Herdtweck, C. Hecht, *J. Organomet. Chem.* **1986**, *314*, 295.
- [11] H. Brunner, L. Poll, J. Wachter, *Polyhedron* **1996**, *15*, 573.
- [12] O. Blacque, M. M. Kubicki, J. Wachter, in preparation for *New J. Chem.*
- [13] W. Hönlle, C. Wibbelmann, W. Brockner, *Z. Naturforsch.* **1984**, *39b*, 1088.
- [14] T. J. Bastow, H. J. Whitfield, *J. Chem. Soc. Dalton Trans.* **1973**, 1739.
- [15] a) T. Ito, N. Morimoto, R. Sadanaga, *Acta Crystallogr.* **1952**, *5*, 775; b) D. J. E. Mullen, W. Nowacki, *Z. Kristallogr.* **1972**, *136*, 48; c) E. J. Porter, G. M. Sheldrick, *J. Chem. Soc. Dalton Trans.* **1972**, 1347.
- [16] M. Drieß, R. Janoschek, H. Pritzkow, *Angew. Chem.* **1992**, *104*, 449; *Angew. Chem. Int. Ed. Engl.* **1992**, *31*, 460.
- [17] C. von Hänisch, D. Fenske, F. Weigend, R. Ahlrichs, *Chem. Eur. J.* **1997**, *3*, 1494.
- [18] a) C. H. E. Belin, M. M. Charbonnel, *Inorg. Chem.* **1982**, *21*, 2504; b) M. Ansari, J. A. Ibers, S. C. O'Neal, W. T. Pennington, J. W. Kolis, *Polyhedron* **1992**, *11*, 1877; c) W. Czado, U. Müller, *Z. Anorg. Allg. Chem.* **1998**, *628*, 239; d) D. M. Smith, M. A. Pell, J. A. Ibers, *Inorg. Chem.* **1998**, *37*, 2340.
- [19] R. D. Harcourt, *J. Mol. Struct. (Theochem)* **1990**, *206*, 253.
- [20] O. J. Scherer, G. Kemény, G. Wolmershäuser, *Chem. Ber.* **1995**, *128*, 1145.
- [21] a) L. Y. Goh, W. Chen, R. C. S. Wong, Z.-Y. Zhou, H. K. Fun, *Mendeleev Commun.* **1995**, 60; b) L. Y. Goh, W. Chen, R. C. S. Wong, *Organometallics* **1999**, *18*, 306.
- [22] M. Noel, K. I. Vasz, *Cyclic Voltammetry and the Frontiers of Electrochemistry*, Aspect Publications, London, **1990**.
- [23] O. J. Scherer, S. Weigel, G. Wolmershäuser, *Chem. Eur. J.* **1998**, *4*, 1910.
- [24] a) Y. Morino, T. Ukaji, T. Ito, *Bull. Chem. Soc. Jpn.* **1966**, *39*, 71; b) R. Enjalbert, J. Galy, *Acta Crystallogr. Sect. B* **1980**, *36*, 914.
- [25] C. A. Ghilardi, S. Midollini, S. Moneti, A. Orlandini, *J. Chem. Soc. Chem. Commun.* **1988**, 1241.
- [26] A recently performed crystal structure analysis of **3** shows identical results (M. Zabel, personal communication; F. Leis, Thesis, Universität Regensburg, **2000**).
- [27] E. Samuel, D. Guery, J. Vedel, *J. Organomet. Chem.* **1984**, *263*, C43.
- [28] M. E. Barr, L. F. Dahl, *Organometallics* **1991**, *10*, 3991.
- [29] O. J. Scherer, M. Swarowsky, G. Wolmershäuser, *Angew. Chem.* **1988**, *100*, 423; *Angew. Chem. Int. Ed. Engl.* **1988**, *27*, 405.

- [30] O. J. Scherer, K. Pfeiffer, G. Heckmann, G. Wolmershäuser, *J. Organomet. Chem.* **1992**, *425*, 141.
- [31] a) H. Brunner, A. Merz, J. Pfauntsch, O. Serhadli, J. Wachter, M. L. Ziegler, *Inorg. Chem.* **1988**, *27*, 2055; b) H. Ogino, H. Tobita, S. Inomata, M. Shimoi, *J. Chem. Soc. Chem. Commun.* **1988**, 586.
- [32] a) O. J. Scherer, G. Schwarz, G. Wolmershäuser, *Z. Anorg. Allg. Chem.* **1996**, *622*, 951; b) O. J. Scherer, T. Hilt, G. Wolmershäuser, *Organometallics* **1998**, *17*, 4110.
- [33] a) K. Wade, *Adv. Inorg. Chem. Radiochem.* **1976**, *18*, 1; b) D. M. P. Mingos, R. L. Johnston, *Struct. Bonding* **1987**, *68*, 29.
- [34] Gaussian 94, Revision E.1, Gaussian, Inc., Pittsburgh PA, **1995**.
- [35] a) R. Hoffmann, W. N. Lipscomb, *J. Chem. Phys.* **1962**, *36*, 2872; b) C. Mealli, D. M. Proserpio, *J. Chem. Educ.* **1990**, *67*, 399.
- [36] a) J. W. Lauher, M. Elian, R. H. Summerville, R. Hoffmann, *J. Am. Chem. Soc.* **1976**, *98*, 3219; b) E. D. Jemmis, A. C. Reddy, *Organometallics* **1988**, *7*, 1561; c) W. Tremel, R. Hoffmann, M. Kertesz, *J. Am. Chem. Soc.* **1989**, *111*, 2030.
- [37] C. Mealli, F. Costanzo, A. Ienco, M. Peruzzini, E. Perez-Carreno, *Inorg. Chim. Acta* **1998**, *275*, 366.
- [38] H. Brunner, F. Leis, B. Nuber, J. Wachter, *Polyhedron* **1998**, *18*, 347.
- [39] S. C. O'Neal, W. T. Pennington, J. W. Kolis, *J. Am. Chem. Soc.* **1991**, *113*, 710.
- [40] Crystallographic data of **1**, **2** and **4** (excluding structure factors) have been deposited with the Cambridge Crystallographic Data Centre as supplementary publication nos. CCDC-143349 (**1**), -143350 (**2**) and -143351 (**4**). Copies of the data can be obtained free of charge on application to CCDC, 12 Union Road, Cambridge CB21EZ, UK (fax: (+44)1223-336-033; e-mail: deposit@ccdc.cam.ac.uk).

Received: May 11, 2000

Revised version: October 23, 2000 [F2479]